NANO-ZERO VALENT IRON ON GEOTHERMAL SILICATE SUPPORT FOR THE REDUCTION OF NITRATE

H. Putri Fraser, James H Johnston, and J. Robin Fulton

School of Physical and Chemical Sciences, Victoria University of Wellington, P.O. Box 600, Wellington 6140, New Zealand

putri.fraser@vuw.ac.nz

Keywords: *nZVI, geothermal silicate, nitrate reduction, surface modification.*

ABSTRACT

Nitrate is one of the major pollutants in New Zealand waterways. Nano-zero valent iron (nZVI) has previously been used to reduce nitrate to ammonia with some success. However, as nZVI is inherently magnetic, these particles tend to agglomerate. Agglomerated nanoparticles lose some of their effectiveness due to the reduction of their surface area. Agglomeration also impedes the mobility of the particles within soils. Paradoxically, as nano particles are highly reactive, it is imperative to ensure that the particles are well contained and not loose in the environment.

One method to circumvent the shortcomings of nanoparticles for environmental application is to use an inert support material. Ideally, nano particles adsorb evenly on the surface of the support, hence maintaining surface area and reactivity, while reducing the agglomeration of the material.

Microsilica 600, a silica fume from the Rotorua geothermal area (Golden Bay Cement) has been used as an additive for cementitious material due to its pozzolanic nature. Raw Microsilica 600 was not an effective support for nZVI. A series of treatments were developed, and these enabled the nZVI particles to be adsorbed successfully on the Microsilica surface.

The reactivity of these hybrid materials were tested with 10 mg dm^{-3} nitrate (as N) on lab scale experiments, and they were successful in reducing 90% of the nitrate into ammonia within 60 minutes. The success of the reduction depends on both the evenness of the adsorption of nZVI and the presence of FeOOH coating on the silica surface. Furthermore, the supported nZVI are able to travel deeper into the soil, making the supported nZVI more effective as a nitrate reductant.

1. INTRODUCTION

1.1Nitrate pollution

Nitrogen is vital to all life. Plants and microorganisms uptake nitrogen as nitrate (NO_3^-) and ammonium (NH_4^+) ions. However, excess nitrate in waterways accelerates eutrophication (Anderson, 2002). The excess nutrients fuel the growth of algae, cyanobacteria and nuisance weeds. The uncontrolled growth of cyanobacteria, commonly known as a toxic algae bloom, is dangerous due to both the biomass and the toxins they produce. These toxins may cause injuries and mortalities in wild and farmed fish (Biggs, 2000). In humans and other mammals, damage is caused through contact, exposure and ingestion of contaminated water and consumption of shellfish that have ingested toxic algae. The overgrowth of weeds also impairs native fish spawning through habitat alteration. When the algae and weeds die, the rotting masses reduce the amount of dissolved oxygen available in the waterways, which, in turn, reduces the number of fish and other aquatic animals (Biggs, 2000).

Excess nutrients in streams also accelerate terrestrial carbon loss from the stream (Rosemond, 2015). Terrestrial carbon is important in riverine food webs as it acts as food source for aquatic life. Excess nutrients not only encourage accumulation of carbon in weeds, but it also encourages mineralisation of organic carbon, which in turn releases carbon as CO_2 to the atmosphere.

Nitrate is also toxic to fish at concentrations as low as 0.8 mg dm^{-3} nitrogen as nitrate (NO_3^--N) (Waikato Regional Council). Excess nitrate in drinking water is also one of the co-factors in methemoglobinemia, or blue-baby syndrome, in infants under four months old.

1.2 Nitrate remediation

In New Zealand, one of the major source of nitrate pollution is fertiliser and effluent run-off from dairy farms. (Statistics NZ; Moir, 2010; Di, 2002) Good farming practices, such as riparian strips planting, waterways fencing, effluent ponds installation, and optimum fertiliser application may reduce nitrate leaching (DairyNZ). However, nitrate is a highly soluble ion and cannot be effectively retained by soil, and therefore tend to leach with any rain event.

In wastewater treatment plants, nitrate is typically sequestered using various method including ion exchange (Bae, 2002; An, 2011), electrodialysis (Elmidaoui, 2001; Hell, 1998), reverse osmosis (Schoeman, 2003) and adsorption (Bhatnagar, 2010; Mizuta, 2004; Teimouri, 2016; Öztürk, 2004) The major drawback of nitrate sequestration is the production of concentrated nitrate brine that needs to be treated separately.

Nitrate is a stable ion with limited reactivity. However some soil bacteria or chemicals can reduce nitrate to various ions and compounds such as nitrogen dioxide (NO_2), nitrite (NO_2^-), nitric oxide (NO), nitrous oxide (N_2O), dinitrogen (N_2) and ammonia/ammonium (NH_3 / NH_4^+). (Moorman, 2010) N_2 is the most desirable product as it is harmless, followed by NH_3/NH_4^+ as it can be utilised by plants. NO_2, NO and N_2O are potent greenhouse gasses and may cause acid rain, while NO_2^- can easily oxidised back to NO_3^- and hence these compounds are not desirable by-product of nitrate reduction. Well maintained bioreactors, for example, may release N_2 instead of the more toxic N_2O. (Moorman, 2010; Schipper, 2001). Maintenance of bioreactors includes periodic flushing and removal of biomass produced.

Chemical reduction of nitrate can be accomplished using various reductants such as sodium borohydride ($NaBH_4$) (Fanning, 2000), formic acid (HCOOH) (Nakamura, 1978), and hydrogen gas (H_2) (Pintar, 2001), all in the presence of various metal catalysts such as copper, zinc, tin and palladium. Another reductant of note is nano-sized elemental solid iron (nano zero valent iron/nZVI), that reduce nitrate to ammonium (Liu, 2012). The advantage of iron over other chemical reductant is that iron is ubiquitous in the environment, and hence it does not add other possible pollutant to the environ. As iron can only reduce nitrate to ammonia, its application is more suited to soil rather than waterways. The hydrogen bonds of ammonium means that it can be retained by soil structure and used as fertiliser (Uexküll, 1995).

As with other solid reagents, the smaller the particle size, the more reactive the reagents is. The total surface area increases as the particle size gets smaller, increasing the amount of reaction sites (Silbeberg, 2009). nZVI is inherently magnetic and thus agglomerate readily. Agglomeration reduce surface area, thus reducing the reactivity of nZVI (Greenlee, 2012) Furthermore, the agglomeration hinders the mobility of nZVI in soil structure, reducing the volume of soil that can be treated. (Li, 2011)

One method to reduce the agglomeration of nZVI is to adsorb the nanoparticles onto larger particles (Meeks, 2012). As these are to be applied to soil then it is imperative that the support particles are non-toxic. As silica and silicate are naturally abundant in soil, a series of silica and silicate from various sources such as silica fume, fumed silica, fly ash, synthetic silica and ground glass were trialled as support material. Microsilica 600, as supplied Golden Bay Cement was found to be the most promising and hence used for this project. Some adsorption can be seen on the surface of microsilica 600, but more surface modification were required to ensure no nanoparticles is loose when the system is deployed.

Overall, there are four surface modification methods applied. First is calcination, as this alters the activity and presence of silanol chemical functionality that regulate the reactivity of the silica surface. Acid washing was also tried as microsilica 600 is a natural product and acid washing removes metal ions or sulfides present on the surface. Activation by boiling is also applied to regenerate any silanol lost during calcination. The surface was also modified by adding an FeOOH (iron oxyhydroxide) layer to increase the surface charge and attraction to zero valent iron.

2. EXPERIMENTAL

2.1 Surface modification

As reported by Golden Bay Cement, microsilica 600 (Misi) is an amorphous silica from hydrothermally altered rhyolitic rocks, that has been extensively altered by silification. Powder XRD analysis shows that Misi contains crystalline form of both quartz and cristobalite, along with greigite. The surface area of Misi was measured as 17.53 (± 0.04) m^2/g, with a pore size of 161 Å. The zeta potential of microsilica 600 remained negative (-50 to -10 mV) between pH 1.5 to 12.

Combinations of surface modification treatment were conducted to test the effect of each treatment. For calcination. Misi was placed in a furnace at either 400 or 600 °C for 6 hours (denoted as C400 and C600 respectively). Uncalcined microsilica is denoted as uC. Misi was also washed in 5.6 M of HCl, referred to as **5**. Activation by boiling was conducted in millipore water for 2 hours, denoted as activated (A) and non-activated **(**nA). The last modification is the addition of FeOOH layer (F), created by soaking Misi in ferrous salt solution (2:1 SiO_2: $FeSO_4.7H_2O$ $^w/_w$), followed by heating the solids in air (120 °C, 2 hours).

The naming of the product indicates the order of treatment. For example, Misi-C600-5-A-F is Misi that has been calcined at 600 °C for 6 hours, then washed in 5.6M HCl, activated by boiling, and have FeOOH coating added.

2.2 nZVI adsorption

The synthesis of Misi-nZVI was performed under N_2 atmosphere using standard Schlenk techniques. In a typical procedure, 1.0 g of Misi was re-suspended using ~30 mL DI-H_2O and added to a Schlenk flask containing $FeSO_4{\cdot}7H_2O$ (0.5 g, 1.7 mmol). The solution was then deoxygenated by bubbling N_2 through the solution for 15 minutes. A glass coated magnetic stir-bar was used for mixing The Misi/iron suspension was then left to stir for approximately 10 minutes until all the light green $FeSO_4{\cdot}7H_2O$ crystalline solid dissolved. $NaBH_4$ (0.2 g, 5.3 mmol) and deoxygenated DI-H_2O (10 mL) was directly added directly to a 20 mL plastic syringe. Using a syringe pump (NE-1000, New Era Pump System), $NaBH_4$ solution was added to the Misi/iron solution at a rate of 0.2 mL/minute. A black precipitate was observed upon addition of the $NaBH_4$ solution. After the addition of all $NaBH_4$ solution, the mixture was left to stir for another 10 minutes. The resulting magnetic particles were separated using a strong magnet, and the liquor removed via cannula. The precipitate was then washed twice with ~50 mL deoxygenated DI-H_2O, then with ~50 mL of deoxygenated EtOH. The particles were then dried under vacuum.

Adsorption of nZVI onto Misi surface were examined using SEM. All SEM images were taken under high vacuum with a JEOL 6500F SEM. The accelerating voltage used was either 15 kV (SEI only) or 20 kV (SEI and EDS). Working distance used was 9-10 mm. Samples were loaded on carbon tape placed on an 1 cm aluminium stub, vacuum dried for at least 6 hours before being coated with 7-9 nm carbon using Quorum Q150T E carbon coater prior to use.

2.3 Nitrate reduction

To prepare a 100 ppm NO_3^--N solution, oven-dried (105 °C, 24 hour) KNO_3 (0.7218 g, 7.100 mmol) was made up to a 1.000 L solution with DI-H_2O in a volumetric flask. A 10 ppm NO_3^--N solution was prepared by quantitative dilution of the 100 mg dm^{-3}.

In a typical nitrate reduction experiment, 100 mL of 10 ppm KNO_3 was deoxygenated and 1.0 g of Misi-nZVI particles was added under N_2 atmosphere and the suspension was stirred continuously using a glass-coated magnetic stir bar. Aliquots (3 - 5 mL) were taken at set time points. The aliquots were passed through a 0.25 μm acetate cellulose syringe filter to remove the particulates. For a typical Misi-nZVI system containing a nominal 10% nZVI, the molar ratio of NO_3^- to Fe was 1:25.

Two methods were employed to quantify nitrate: UV-Vis spectroscopy and ion chromatography. The spectra were obtained using a Cary Bio-50 spectrophotometer at 220 nm (ε (NO_3^-) = 5.161 x 10^{-3} mol/dm^2). Using a quartz cuvette, the concentration of nitrate was quantified against a known standard curve from about 0.1 - 10 ppm range.

For ion chromatography, approximately 5 mL of sample were passed through 0.25 μm acetate cellulose syringe filters into a PolyVial^{TM} and capped. The samples were loaded to an autosampler along with at least 3 known standards that cover both the low and high end of possible nitrate concentration. A Thermofisher IC 1100 was used with Dionex IonPac AS14 column, Dionex IonPac AG 14 column guard, Dionex AERS 500 suppressor and injection volume of 25μL. The eluent used was Dionex AS23 Eluent concentrate, diluted to 3.5 mM Na_2CO_3/1 mM $NaHCO_3$.

3. RESULTS

3.1 Surface modification

The surface area of Misi decreased upon calcination to 600 °C, from 17.53 m^2/g to 11.66 m^2/g. Calcination at 400 °C did not produce a significant change in surface area (17.42 m^2/g). The data suggested a collapse and coalescence of the silicate structure at 600 °C; however this could not be detected in SEM analysis of the material.

Washing with 5.6 M acid reduced the surface area of raw Misi to 14.92 m2/g from 17.53 m2/g (Table 1). This was in contrast to acid treatment (10M HCl) of silica gel in which the surface was reported to stay the same. However, the surface area of various acid treated clays such as bentonite, biotite, kaolin and vermiculite increased by as much as 3.5 times (5M HCl, r.t., 2 weeks). These reported results correspond to the metal content of each system: silica gel has less than 0.04 % metal impurities, while clay contains varying degree of metal, from 0.2 % (kaolin) to 2.8 % in biotite.

Table 1. Surface area of acid washed and calcined microsilica

Silicate	Surface area (m^2/g)
Raw Misi	17.53 (± 0.04)
Misi-5	14.99 (± 0.07)
Misi-5-C400	18.9 (± 0.6)
Misi-5-C600	17.1 (± 0.2)

When the calcination was conducted after acid wash, the surface area increased again, especially when calcined at 400 °C. SEM analysis to the acid washed Misi revealed that pits were formed on the surface upon exposure to 5.6 M HCl. No visible changes were observed upon acid washing with either 1.1 or 2.8 M HCl

In a typical synthesis, 100 mg of Fe in the form of $FeSO_4$ (0.5 g $FeSO_4{\cdot}7H_2O$, 98% purity) were added to each gram of Misi to form the FeOOH layer. The presence of extra iron after FeOOH layer formation was confirmed by AAS, with the increase in digestible iron from 620 μg per gram in Misi-C600 to 7.02 mg/g in Misi-C600-AF. This means only 7% of Fe added were adsorbed onto the Misi surface prior to oxidation into FeOOH.

The XRD spectrum of Misi-C600-AF did not reveal any additional crystalline material compared to Misi C600 (Figure 1). Lepidocrocite (γ-FeOOH) and goethite (α-FeOOH) were shown as reference as goethite is the expected phase of FeOOH formed under this condition while lepidocrocite can often be formed from goethite under oxidation and with the presence of carbonate. The presence of either material could not be confirmed and this could be due to the relatively small amount of FeOOH compared to Misi.

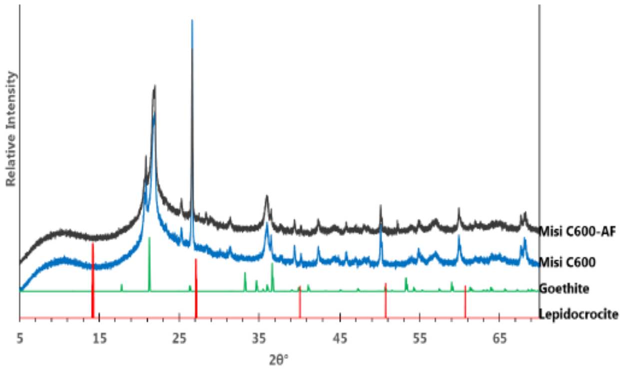

Figure 1: Powder X-Ray diffraction of Misi-C600 compared to Misi C600-AF with reference of goethite (RRUFF ID: R120086) and lepidocrocite (RRUFF ID: R050454)

Qiu (2011) stated that one of the aims of coating silica surface with FeOOH was to increase surface area of the silica to allow more nucleation sites. The surface area of FeOOH-coated Misi was analysed and found to correlate with the order of treatment. When the silicate had not been washed in acid, the surface area increased with FeOOH coating. However, washing in acid changed this relationship as the acid soak reduced surface area (Table 2, entry 1 and 6). Calcination after acid washing increased the surface significantly (compare entry 7 and 9 to 2 and 4). The addition of FeOOH layer decreased surface area when the silica had been acid-washed. A plausible explanation was that acid washing allows access to the interior of the particles that were removed during calcination; and as silicate were coated with FeOOH the surface area was reduced due to the adsorption of FeOOH in the silicate interior.

Table 2. Surface area of treated and untreated Misi

Entry	Silicate	Surface Area (m^2/g)
1	Raw Misi	17.53 (± 0.04)
2	Misi-C400	17.12 (± 0.03)
3	Misi-C400-AF	17.28 (± 0.09)
4	Misi-C600	16.66 (± 0.05)
5	Misi-C600-AF	19.05 (± 0.04)
6	Misi-5	14.99 (± 0.07)
7	Misi-5-C400	18.9 (± 0.6)
8	Misi-5-C400-AF	17.4 (± 0.1)
9	Misi-5-C600	17.1 (± 0.2)
10	Misi-5-C600-AF	13.9 (± 0.03)
11	Misi-C600-5-AF	17.36 (± 0.06)

3.2 nZVI adsorption

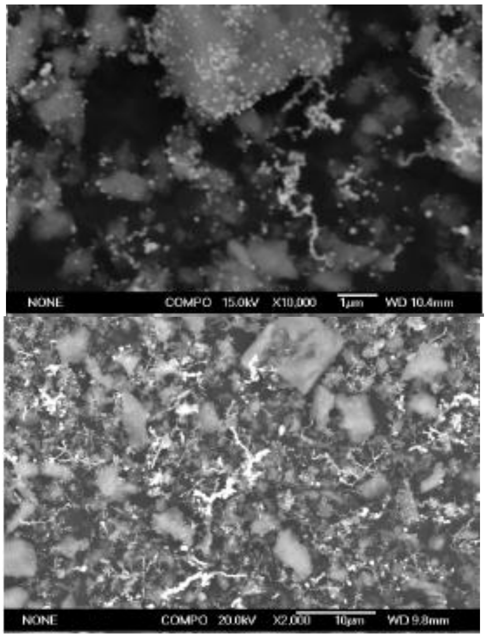

Figure 2. Effect of calcination on nZVI adsorption on Misi. a) Calcined: Misi-5-C600-AF-nZVI, b) uncalcined: Misi-5-uC-AF-nZVI

Calcination is an important step in modifying Misi surface for nZVI absorbance. Uncalcined Misi did not adsorb nZVI when other treatment, including acid washing or addition of FeOOH coating, were applied (Figure 2).

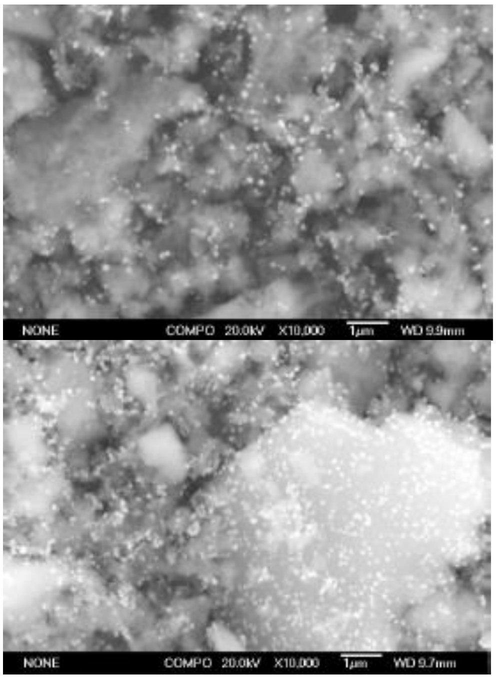

Figure 3. Effect of calcination temperature on nZVI adsorption on Misi a) 400 °C: Misi-C400-5-AF-nZVI b) 600 °C: Misi C600-5-AF-nZVI.

Calcination either at 400 °C or 600 °C had similar effects on nZVI adsorption by Misi, while holding the other treatments the same (Figure 3). From this, it seemed that the adsorption of Misi was not related to the presence of greigite that is typically removed by calcination at 600 °C but not at 400 °C, although it might be related to the isolated silanol groups that were generated at 400 and 600 °C. Acid washing can generate weakly acidic functional groups, while calcination creates isolated silanols, thus this suggested that adsorption of nZVI onto Misi surfaces was enhanced by the presence of these functional groups.

Activation by boiling and FeOOH layer were not necessary for good adsorption of nZVI. It was plausible that the combination of acid wash and calcination was enough to create good adsorption sites through the creation of isolated silanol sites.

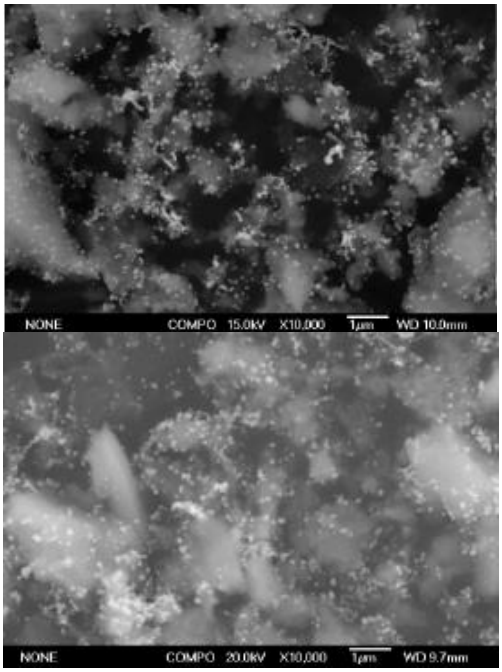

Figure 4. Effect of activation by boiling and FeOOH layer on nZVI adsorption on Acid washed and calcined Misi: a)activated, but no FeOOH: Misi-5-C600-A-nF-nZVI b). not activated, with FeOOH layer : Misi-5-C600-nA-F-nZVI

3.3 Nitrate reduction

The calcination of Misi was an important step for maximizing the adsorption of nZVI onto its surface. Although only minor changes in adsorption of nZVI onto Misi were observed when Misi was calcined at 400 °C versus 600 °C, the samples calcined at 600 °C were consistently able to reduce nitrate more than the samples calcined at 400 °C when comparing similar additional treatments. For instance, after 60 minutes, C400-AF-nZVI removed 39 ± 5% of nitrate whereas C600-AF-nZVI removed 62 ± 9 % (Figure 5). A greater difference was observed with 5-C400-AnF-nZVI and 5-C600-AnF-nZVI, with the former removing 33% after 60 minutes and the later 65 ± 8% in the same time frame. As the nZVI adsorbed on Misi calcined at 600 °C was consistently better than the nZVI adsorbed on Misi calcined 400 °C, the rest of the nitrate reduction studies were performed on nZVI adsorbed on Misi calcined at 600 °C. One major difference between Misi C400 and Misi C600 was the presence of greigite. Hence, it was possible that greigite hindered the reduction of nitrate by nZVI, but the reason and mechanism for this inhibition was unclear.

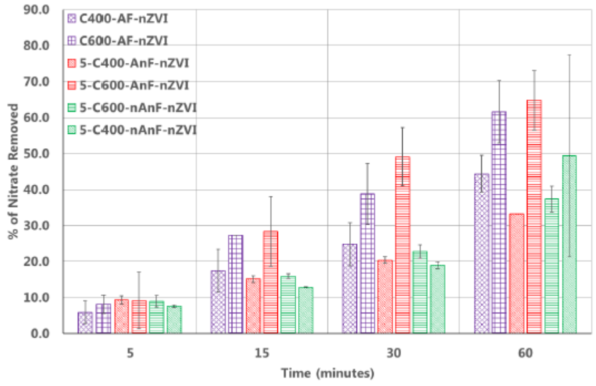

Figure 6. Nitrate reduction by Misi-nZVI that has been calcined at different temperature.

Figure 6 also revealed that additional surface treatment steps might also be important in maximizing the nitrate reduction rate of nZVI. This was more notable in the Misi samples that were not boiled or possess a FeOOH coating (green bars). These results were explored further by comparing the difference in the nitrate reduction rates in the 5-C600 series (Figure 7). The nZVI adsorbed on Misi that had undergone the most treatment reduced nitrate faster than all other samples, with 90 ± 14% reduced after 60 minutes. The FeOOH coating had a greater effect on nitrate reduction than boiling (74 ± 12 % and 65 ± 8 % after 60 minutes, respectively).

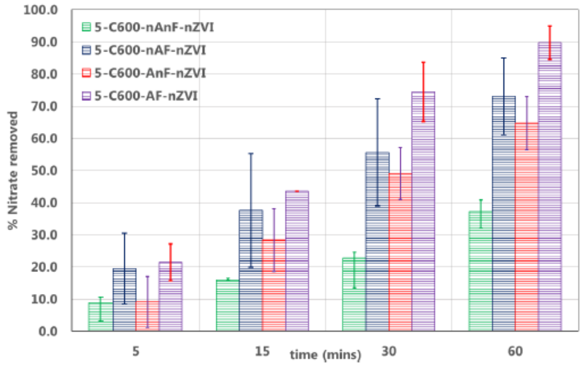

Figure 7. Nitrate reduction by Misi-nZVI on the 5-C600 series.

A similar trend can also be observed in the C600-5 series where Misi was washed with 5.6 M HCl after calcination (Figure 8). nZVI adsorbed on nAnF Misi had a low average with large variability in its nitrate reduction capability (33 ± 26 %). nZVI adsorbed on C600-5-AnF and C-5-AF had similar nitrate reduction capabilities of 80 ± 12% and 85 ± 14 % at 60 minutes, respectively. Whilst the C600-5 series showed the full AF treatment trending to be higher in its nitrate reduction capability, for the C600 series, the reverse was observed. C600-AF-nZVI showed a lower percentage of nitrate removed in 60 minutes compared to C600-nAF-nZVI, though the average was still within the uncertainty limit (62 ± 9% and 70 ± 11 % respectively).

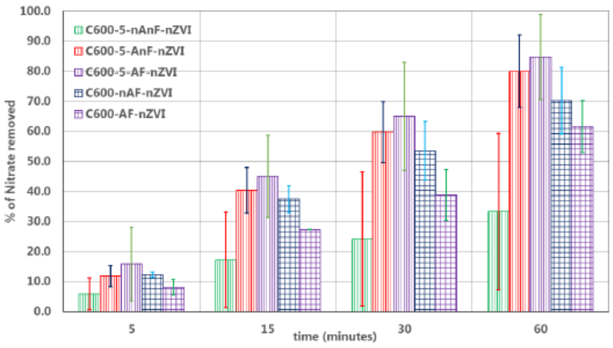

Figure 8. Nitrate reduction by Misi-nZVI in the C600 series.

3.3.1 The role of FeOOH layer on nitrate reduction

The FeOOH layer had little effect on nZVI adsorption, however, the presence of FeOOH seemed to improve nitrate reduction. This improved ability might be explained by the interplay between the FeOOH layer, the oxidation product of nZVI (Fe^{2+}) and Fe_3O_4. In a study by Klausen (1995) , it was found that Fe^{2+} did not have a strong reductive capability, but in the presence of Fe^{3+} containing minerals such as magnetite, lepidocrocite or goethite, the Fe^{2+} reductive capability was increased. This was possibly due to the regenerative ability of the Fe^{3+} containing mineral in providing more Fe^{2+}.

In another study by Gorski (2016), it was found that that in the presence of iron oxides (e.g.goethite and hematite), the redox couple of Fe^{3+}/Fe^{2+} had a lower standard reduction potential, especially at higher pH. A ‘normal’ standard reduction potential of Fe^{3+}/Fe^{2+} was 771 mV. In the presence of goethite the reduction potential was 768 ± 1 mV, while in the presence of hematite, the reduction potential was 739 ± 16 mV, thus indicating a stronger reducing power of Fe^{2+} in the presence of these minerals. In the presence of nZVI, Fe^{2+} promoted the reduction of nitrate through the formation of Fe_3O_4. (Gorski, 2016) While Fe^0 served as electron donors to reduce nitrate, the reduction of Fe^0 and Fe^{2+} to Fe_3O_4 also provided both electron and protons that acted as a buffer for the reaction and maintain the pH at 7. Furthermore, Fe_3O_4 is a good electrical conductor, effectively lowering the electrical resistance and assisting with electron transfer from the Fe^0 to nitrate.

3.3.2. The role of acid washing on nitrate reduction

Acid washing reduced the surface area of Misi (Table 1). Upon calcination however, the surface area of Misi increased again. The role of acid washing and calcination on nitrate reduction was not clear, however there were some possible explanations. First, the acid washing removes metal impurities, which allows FeOOH to form on all available surfaces. This increase in FeOOH formation allows improved reduction of nitrate. Second, the acid washing along with activation, allowed the formation of more reactive silanol sites. This allowed better dispersion of nZVI), and hence better reduction.

4. CONCLUSION

All of the Misi-supported nZVI material were able to reduce nitrate, although none were as effective as bare nZVI. The reduction rate was fastest when Misi had undergone all of the surface modifications investigated, including calcination, acid washing, boiling and coating with FeOOH. There was no correlation between the nitrate reduction rate and the A-value, indicating that nZVI adsorption alone was not the determining factor in the reduction of nitrate. Instead, it was the cumulative effect of all the treatments that work together to generate a reactive system.

5. ACKNOWLEDGMENTS

This work was partially funded by Todd Foundation Scholarship and Curtis-Gordon Scholarship.

6. REFERENCES

An, B., Liang, Q., & Zhao, D. . *Removal of arsenic(V) from spent ion exchange brine using a new class of starch-bridged magnetite nanoparticles.* Water Research, 45(5), 1961–1972. (2011)

Anderson, D. M., Glibert, P. M., & Burkholder, J. M. *Harmful algal blooms and eutrophication: Nutrient sources, composition, and consequences*. Estuaries, 25(4), 704–726. (2002)

Bae, B.-U., Jung, Y.-H., Han, W.-W., & Shin, H.-S. . *Improved brine recycling during nitrate removal using ion exchange.* Water Research, 36(13), 3330–3340. (2002)

Bhatnagar, A., Kumar, E., & Sillanpää, M. *Nitrate removal from water by nano-alumina: Characterization and sorption studies.* Chemical Engineering Journal, 163(3), 317–323. (2010)

Biggs, B. J. F. *New Zealand Periphyton Guideline: Detecting, Monitoring and Managing Enrichment of Streams.* National Institute of Water and Atmospheric Research.(2000)

DairyNZ. . *Sustainable Dairy Water Accord.* Retrieved February 23, 2015, from http://www.dairynz.co.nz/media/209792/Sustainable-Dairying-Water-Accord.pdf (n.d.)

Di, H. J., & Cameron, K. C. *Nitrate leaching in temperate agroecosystems: sources, factors and mitigating strategies.* Nutrient Cycling in Agroecosystems, 64(3), 237–256. (2002)

Elmidaoui, A., Elhannouni, F., Sahli, M. A. M., Chay, L., Elabbassi, H., Hafsi, M., & Largeteau, D. *Pollution of nitrate in Moroccan ground water: removal by electrodialysis.* Desalination, 136, 325–332 (2001)

Fanning, J. C. *The chemical reduction of nitrate in aqueous solution.* Coordination Chemistry Reviews, 199(1), 159–179. (2000)

Gorski, C. A., Edwards, R., Sander, M., Hofstetter, T. B., & Stewart, S. M. *Thermodynamic Characterization of Iron Oxide–Aqueous* Fe^{2+} *Redox Couples.* Environmental Science & Technology, 50(16), 8538–8547. (2016)

Greenlee, L. F., & Hooker, S. A. *Development of stabilized zero valent iron nanoparticles.* Desalination and Water Treatment, 37(1–3), 114–121. (2012).

Hell, F., Lahnsteiner, J., Frischherz, H., & Baumgartner, G. . *Experience with full-scale electrodialysis for nitrate and hardness removal*. Desalination, 117(1), 173–180. (1998)

Klausen, J., Troeber, S. P., Haderlein, S. B., & Schwarzenbach, R. P. *Reduction of Substituted Nitrobenzenes by Fe(II) in Aqueous Mineral Suspensions.* Environmental Science & Technology, 29(9), 2396–2404. (1995)

Li, Y., Li, T., & Jin, Z. *Stabilization of Fe0 nanoparticles with silica fume for enhanced transport and remediation of hexavalent chromium in water and soil.* Journal of Environmental Sciences, 23(7), 1211–1218. (2011).

Liu, H. B. B., Chen, T. H. H., Chang, D. Y. Y., Chen, D., Liu, Y., He, H. P. P., Frost, R. *Nitrate reduction over nanoscale zero-valent iron prepared by hydrogen reduction of goethite.* Materials Chemistry and Physics, 133(1), 205–211. (2012).

Meeks, N. D., Smuleac, V., Stevens, C., & Bhattacharyya, D. *Iron-Based Nanoparticles for Toxic Organic Degradation: Silica Platform and Green Synthesis.* Industrial & Engineering Chemistry Research, 51(28), 9581–9590.(2012).

Mizuta, K., Matsumoto, T., Hatate, Y., Nishihara, K., & Nakanishi, T. *Removal of nitrate-nitrogen from drinking water using bamboo powder charcoal.* Bioresource Technology, 95(3), 255–257. (2004)

Moir, J. , Cameron, K. C., Di, H. ., & Ferstak, U. *The spatial coverage of dairy cattle urine patches in an intensively grazed pasture system.* Journal of Agricultural Science, 1–13. (2010)

Moorman, T. B., Parkin, T. B., Kaspar, T. C., & Jaynes, D. B. *Denitrification activity, wood loss, and* N_2O *emissions over 9 years from a wood chip bioreactor.* Ecological Engineering, 36(11), 1567–1574 (2010)

Nakamura, H., Yamaguchi, I., & Kubota, M. *Effect of Platinum Group Elements on Denitration of High-Level Liquid Waste with Formic Acid.* Journal of Nuclear Science and Technology, 15(10), 760–764. (1978)

Öztürk, N., & Bektaş, T. E. *Nitrate removal from aqueous solution by adsorption onto various materials.* Journal of Hazardous Materials, 112(1), 155–162. (2004)

Pintar, A., Batista, J., & Levec, J. *Integrated ion exchange/catalytic process for efficient removal of nitrates from drinking water.* Chemical Engineering Science, 56(4), 1551–1559. (2001).

Qiu, X., Fang, Z., Liang, B., Gu, F., & Xu, Z. *Degradation of decabromodiphenyl ether by nano zero-valent iron immobilized in mesoporous silica microspheres.* Journal of Hazardous Materials, 193, 70–81 (2011)

Rosemond, A. D., Benstead, J. P., Bumpers, P. M., Gulis, V., Kominoski, J. S., Manning, D. W. P., Wallace, J. B. *Experimental nutrient additions accelerate terrestrial carbon loss from stream ecosystems.* Science, 347(6226), 1142–1145. (2015)

Schipper, L. A., & Vojvodić-Vuković, M. *Five years of nitrate removal, denitrification and carbon dynamics in a denitrification wall.* Water Research, 35(14), 3473–3477. (2001).

Schoeman, J. J., & Steyn, A. *Nitrate removal with reverse osmosis in a rural area in South Africa*. Desalination, 155(1), 15–26. (2003)

Silbeberg, M. S. *Chemistry: The Molecular Nature of Matter and Change (5th ed.).* New York: McGraw-Hill.(2009).

Statistics NZ. (n.d.). *Fertiliser Use and the Environment.* Retrieved February 18, 2015, from http://www3.stats.govt.nz/environment/Fertiliser_use_and_the_environment_Aug06.pdf

Teimouri, A., Nasab, S. G., Vahdatpoor, N., Habibollahi, S., Salavati, H., & Chermahini, A. N. *Chitosan /Zeolite Y/Nano* ZrO_2 *nanocomposite as an adsorbent for the removal of nitrate from the aqueous solution.* International Journal of Biological Macromolecules, 93, 254–266. (2016)

Uexküll, H. R., & Mutert, E. *Global extent, development and economic impact of acid soils.* Plant and Soil, 171(1), 1–15. (1995).

Waikato Regional Council. (n.d.). *Water quality glossary*. Retrieved February 20, 2015, from http://www.waikatoregion.govt.nz/Environment/Natural-resources/Water/Rivers/healthyrivers/Water-quality-glossary/